Simultaneous detection of multiple metal ions using a single ^{19}F-iCEST probe

Amnon Bar-Shir[1,2], Nirbhay N Yadav[1,3], Assaf A Gilad[1,2], Peter CM van Zijl[1,3], Michael T McMahon[1,3], and Jeff WM Bulte[1,2]

[1]*Russell H. Morgan Department of Radiology and Radiological Science, the Johns Hopkins University School of Medicine, Baltimore, MD, United States,* [2]*Cellular Imaging Section, Institute for Cell Engineering, the Johns Hopkins University School of Medicine, Baltimore, MD, United States,* [3]*F.M. Kirby Research Center for Functional Brain Imaging, Kennedy Krieger Institute, Baltimore, MD, United States*

Target Audience: Scientists and clinicians who are interested in molecular and cellular imaging, especially those who are interested in the detection of low concentration metal ions using MRI, those developing new methods for CEST MRI, and those developing new contrast agents for ^{19}F MRI.

Purpose: To extend the previously developed ion-CEST (iCEST) method[1] to simultaneous monitoring of changes in levels of multiple biologically relevant metal ions with high specificity. We hypothesized that different metal ions exhibit different exchange properties with a fluorinated chelate and that the observed chemical shift offset (Δω) between free and metal ion-bound chelate in the ^{19}F-NMR spectrum is unique for each metal, allowing simultaneous "multi-color" imaging of multiple metal ions using saturation transfer-based approach in ^{19}F-MRI framework.

Methods: Experiments were performed on solutions containing 5,5', 6,6'-tetrafluoro-BAPTA (TF-BAPTA, AG Scientific, Inc.) and multiple biologically relevant metal ions (K^+, Na^+, Ca^{2+}, Mg^{2+}, Cu^{2+}, Fe^{2+} and Zn^{2+}) at 37ºC and pH=7.4. *MR Spectroscopy*: TF-BAPTA was dissolved to a final concentration of 5 mM, and ions were add at 500 μM. Using 5-Fluorocytosine (5-FC) as an internal ^{19}F reference, ^{19}F-NMR spectra were acquired (11.7 T NMR spectrometer, Bruker). *MRI*: Experiments were performed on a 17.6 T MRI scanner (Bruker). TF-BAPTA was dissolved to 10 mM with 200 μM of ion. A RARE (factor 8) sequence was used to acquire ^{1}H MRI (TR/TE=5,000/7.7 ms, 1 mm slice, FOV=2×2 cm, matrix size=128×128). For ^{19}F MRI, the center frequency (O_1) was set at the frequency of the ^{19}F atom at the 6 position (0.0 ppm) of TF-BAPTA (**Fig. 1a**), while signal from the ^{19}F located at the 5 position of TF-BAPTA (**Fig. 1a-b**, 4.5 ppm downfield) was suppressed. A modified RARE sequence (TR/TE=4,000/3.4 ms, RARE factor=16, 6 mm slice, FOV=2×2 cm, matrix size=32×32, and a saturation pulse B_1=1.2, 2.4 or 3.6 μT/ 2 s) were used to acquire ^{19}F iCEST. Mean ^{19}F Z-spectra (iCEST spectra), were obtained after B_0 correction. CEST contrasts, i.e., the magnetization transfer ratio (MTR) images were calculated after Lorentzian line shape fitting[2].

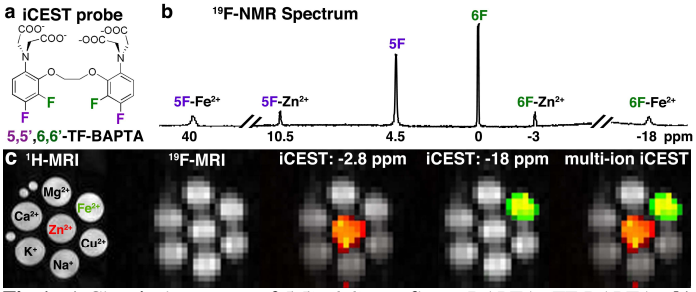

Fig 1. **a)** Chemical structure of 5,5', 6,6'-tetrafluoro-BAPTA (TF-BAPTA). **b)** ^{19}F NMR spectrum (470 MHz) of 5 mM TF-BAPTA in the presence of 0.5 mM Zn^{2+} or Fe^{2+}. **c)** ^{1}H MRI, ^{19}F MRI, and iCEST (Δω=-2.8 ppm or Δω=-18 ppm) overlaid on ^{19}F MRI. The far right shows the ^{19}F multicolor multi-ion iCEST image for 10 mM TF-BAPTA and 200 μM M^{2+} with B_1= 3.6 μT/ 2 s.

Results: **Fig. 1a** illustrates the chemical structure of TF-BAPTA. **Fig. 1b** shows the ^{19}F NMR spectra of TF-BAPTA in the presence of Zn^{2+} or Fe^{2+}, along with the peak assignments. As shown previously for Ca^{2+} binding to TF-BAPTA[3], the downfield NMR peaks (10.5 ppm for Zn^{2+}-TF-BAPTA and 39.5 ppm for Fe^{2+}-TF-BAPTA) are the observed Δωs of the ^{19}F atom at the 5 position (**purple**, **Fig. 1a**), while the upfield Δωs are related to the ^{19}F atom at the 6 position (**green, Fig 1a**). Note that all other examined ions did not reveal additional peaks in the ^{19}F NMR spectrum of TF-BAPTA, except for Ca^{2+} which exchanges too fast (~30,000 s^{-1}) with TF-BAPTA for Δω=9.7 ppm, shifting the peak at the 5 position upon its addition[3]. **Fig. 1c** shows the ^{1}H-MRI and ^{19}F-MRI of 7 tubes containing 10 mM TF-BAPTA and 200 μM of added ion, without any changes in ^{1}H or ^{19}F MR contrast. However, ^{19}F iCEST showed a clear differential MR contrast between the Zn^{2+} and Fe^{2+} containing samples. The iCEST:-2.8 ppm and iCEST:-18 ppm images represent the ^{19}F iCEST contrast obtained when the saturation pulse (B_1=3.6 μM/2 s) was applied at Δω=-2.8 ppm and Δω=-18 ppm, respectively. Theses Δω values were correlated with the Δωs in the ^{19}F NMR spectra upon addition of Zn^{2+} or Fe^{2+}, respectively (see **Fig. 1b**). **Fig. 2a-b** shows the corresponding ^{19}F-iCEST-spectra from the samples containing either Zn^{2+} (**Fig. 2a**) or Fe^{2+} (**Fig. 2b**). The dynamic ion exchange between TF-BAPTA and [M^{2+}-TF-FBAPTA] results in an observed iCEST effect for both ions at Δω=-2.8 ppm for [Zn^{2+}-TF-BAPTA] and at Δω=-18 ppm for [Fe^{2+}-TF-BAPTA]. Using Bloch simulations (solid lines in **Fig. 2a-b**, using a two pool model) the exchange rate (k_{ex}) between free and bound TF-BAPTA is estimated to be ~20 s^{-1} for both ions. Interestingly, when both ions were combined with TF-BAPTA (**Fig 2c**), two distinctive peaks were obtained in the iCEST spectra, which was supported by the Bloch simulations (using a three-pool model). These data confirm that Zn^{2+} and Fe^{2+} can be monitored simultaneously using a single iCEST probe.

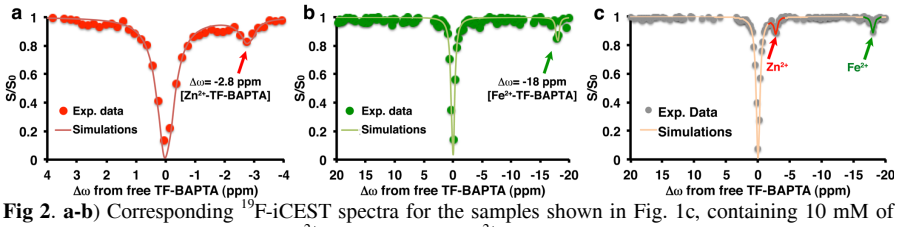

Fig 2. **a-b**) Corresponding ^{19}F-iCEST spectra for the samples shown in Fig. 1c, containing 10 mM of TF-BAPTA and 200 μM of Zn^{2+} (**a**, **red**) and Fe^{2+} (**b**, **green**). Circles represent the average experimental signal, solid lines represent Bloch simulations (two pool model). Arrows point to the Δω of the [M^{2+}-5F-BAPTA] complex. **c**) ^{19}F-iCEST spectra for a sample containing both Zn^{2+} and Fe^{2+} (not shown in Fig. 1), with Bloch simulations (solid line) performed using a three-pool model.

Discussion: The high sensitivity of the ^{19}F NMR spectrum Δω values for changes in chemical environment together with the specificity of these Δωs for certain metal ions allows the development of novel responsive contrast agents for ^{19}F-iCEST. By adding ^{19}F atoms to the 6 position of 5F-BAPTA, which previously allowed only detection of Ca^{2+} using iCEST[1, 4], to obtain TF-BAPTA (**Fig 1a**), it became possible to detect both Zn^{2+} and Fe^{2+}. Adding one ^{19}F atom to the BAPTA backbone dramatically changes the binding properties of TF-BAPTA[3]. At the same time, the added ^{19}F-atom induces k_{ex} values that allow detection of Zn^{2+} and Fe^{2+} with ^{19}F-iCEST MRI. Although other ^{1}H MRI probes for the detection of Zn^{2+} can be used[5], the specificity of iCEST to simultaneously detect different ions using the same sensor represents a new concept for the rational design of novel MRI probes. While the observed k_{ex} between bound and free TF-BAPTA is only 20 s^{-1} for both ions, and higher CEST effect could be obtained for higher k_{ex},[6] we were still able to detect a 200 μM concentration with a 10 mM signal strength. This is due to the nature of iCEST that allows the reduction of the concentration of the ^{19}F-iCEST probe to a detectable molar ratio, a feature that is not available for ^{1}H-CEST, which is based on water. However, further chemical modifications of the fluorinated probe may result in higher k_{ex} and therefore in higher iCEST contrast.

Conclusion: We have extended the ^{19}F iCEST MRI approach by a simple chemical modification of a BAPTA derivative that alters the binding kinetics of metal ions and their chelates, enabling specific and simultaneous detection of Zn^{2+} and Fe^{2+}. While BAPTA derivatives are widely used for fluorescent detection of metal homeostasis *in vitro*, the ability to probe metals non-invasively *in vivo* would have profound implications for the biological sciences.

References: 1. A. Bar-Shir et al., J Am Chem Soc 2013; 135, 12164. 2. C. K. Jones et al., Magn Reson Med 2012; 67, 1579 3. R. E. London et al., Am J Physiol 1994; 266, C1313. 4. H. Gilboa, et al., NMR Biomed 1994; 7, 330. 5. A. J. Lubag et al., PNAS 2011; 108, 18400. 6. P. C. van Zijl, N. N. Yadav, Magn Reson Med 2011; 65, 927. Supported by MSCRFII-0161-00 and MSCRFF-0103-00